Literature Cited

(1) Vijayalakshmi, T. S.; Naidu, P. R. *J. Chem. Eng. Data* **1989**, *34*, 413.
(2) Vijayalakshmi, T. S.; Naidu, P. R. *Indian J. Pure Appl. Phys.* **1990**, *28*, 215.
(3) Rao, M. V. P.; Naidu, P. R. *Can. J. Chem.* **1974**, *52*, 788-90.
(4) Riddick, J. A.; Bunger, W. B. *Techniques of Chemistry*, 3rd ed.; Wiley-Interscience: New York, 1970.
(5) Timmermans, J. *Physico-chemical constants of pure organic compounds*; Elsevier: New York, 1950.

Received for review April 30, 1991. Revised September 17, 1991. Accepted September 26, 1991.

Vapor–Liquid Coexistence Curve and the Critical Parameters of 1-Chloro-1,1-difluoroethane (HCFC-142b)

Seisho Tanikawa, Jun Tatoh, Yukishige Maezawa,* Haruki Sato, and Koichi Watanabe

Department of Mechanical Engineering, Faculty of Science and Technology, Keio University, 3-14-1, Hiyoshi, Kohoku-ku, Yokohama 223, Japan

Vapor–liquid coexistence curve near the critical point of 1-chloro-1,1-difluoroethane (HCFC-142b) was measured by a visual observation of the meniscus in an optical cell. Saturation densities including 13 saturated-vapor and 18 saturated-liquid densities were obtained in the range of temperature from 354 K to the critical temperature, corresponding to the density range from 181 to 947 kg/m^3. The experimental errors in temperature and density were estimated to be within ±10 mK and between ±0.09 and ±0.53%, respectively. Not only the level where the meniscus disappeared but also the intensity of the critical opalescence were considered for the determination of the critical temperature and density as 410.29 ± 0.02 K and 446 ± 3 kg/m^3, respectively. The critical exponent, β, was also determined to be 0.339 ± 0.002. A saturated-vapor/saturated-liquid density correlation was developed on the basis of the present measurements.

Introduction

HCFC-142b (1-chloro-1,1-difluoroethane) is one of the environmentally acceptable refrigerants. A binary mixture of HCFC-22 (chlorodifluoromethane) + HCFC-142b has the possibility of becoming a promising substitute for CFC-12 (dichlorodifluoromethane). We have already reported the critical parameters of several CFC-alternative refrigerants, i.e., HFC-152a (*1*), HFC-134a (*2*), and HCFC-123 (*3*). This paper reports the measured vapor–liquid coexistence curve in the critical region, the experimentally determined critical temperature, density, and exponent, and a saturation density correlation for HCFC-142b.

Experimental Section

A visual observation apparatus, originally built by Okazaki et al. (*4*) and redesigned by Tanikawa et al. (*3*), was used for all measurements. The apparatus and procedure have been reported in detail in our previous publications (*3–6*).

Temperature measurements were performed by using a standard platinum resistance thermometer, and measured temperatures were converted into two different temperature scales of IPTS-68 and ITS-90. All the descriptions given in figures and correlations in the present paper are exclusively dependent on the temperature scale of IPTS-68. The thermometer was put in the vicinity of optical cell at the same level in the bath.

The experimental uncertainty in temperature was estimated to be within ±10 mK as the sum of 2 mK, the precision of the thermometer; 1 mK, the precision of the bridge; and 7 mK, the possible temperature fluctuation of the silicone oil in the bath. The value of the resistance measured with our thermometer at the triple point of water altered by 0.000 03 Ω. The uncertainty in density was estimated to be between ±0.09%, which is considered to be due to the uncertainties of the cell volumes and the sample mass, and ±0.53%, which includes the uncertainty of the expansion factor. The purities of the two samples furnished by manufacturers were 99.8 and 99.9 mass %.

Table I. Saturated-Vapor Densities ρ'' of HCFC-142b[a]

T_{68}/K (T_{90}/K)	ρ''/(kg/m^3)	T_{68}/K (T_{90}/K)	ρ''/(kg/m^3)
395.833 (395.802)	181.3 ± 1.0[b]	408.991 (408.958)	326.3 ± 0.3[b]
399.071 (399.039)	202.8 ± 0.8[b]	409.956 (409.922)	365.5 ± 0.6*[b]
402.747 (402.714)	232.8 ± 0.9[b]	410.232 (410.198)	389.1 ± 0.4*[b]
404.660 (404.627)	252.4 ± 0.4[b]	410.295 (410.261)	412.8 ± 0.8*[b]
405.739 (405.706)	266.9 ± 0.5[b]	410.292 (410.258)	438.0 ± 0.4*[c]
408.218 (408.185)	308.5 ± 0.3[b]	410.293 (410.259)	442.0 ± 0.7*[b]
408.693 (408.660)	318.3 ± 0.5[b]		

[a] Values marked with asterisks are from points at which critical opalescence was observed. [b] Sample with 99.8 mass % purity was used. [c] Sample with 99.9 mass % purity was used.

Table II. Saturated-Liquid Densities ρ' of HCFC-142b[a,d]

T_{68}/K (T_{90}/K)	ρ'/(kg/m^3)	T_{68}/K (T_{90}/K)	ρ'/(kg/m^3)
410.282 (410.249)	446.0 ± 0.4*[c]	403.306 (403.274)	670.8 ± 0.9[b]
410.283 (410.250)	446.8 ± 0.4*[b]	398.562 (398.530)	718.5 ± 0.6[b]
410.290 (410.255)	453.6 ± 0.5*[c]	396.188 (396.157)	738.2 ± 0.7[b]
410.281 (410.248)	473.3 ± 0.5*[b]	391.694 (391.664)	770.2 ± 1.9[b]
410.222 (410.188)	493.5 ± 1.1*[b]	387.434 (387.405)	796.9 ± 1.1[b]
409.645 (409.612)	546.0 ± 0.5[b]	382.291 (382.263)	825.1 ± 1.7[b]
408.450 (408.417)	584.9 ± 1.5[b]	376.617 (376.590)	853.8 ± 0.8[b]
407.686 (407.652)	603.4 ± 1.0[b]	369.842 (369.813)	884.1 ± 1.2[b]
406.465 (406.432)	626.4 ± 1.3[b]	353.548 (353.527)	947.4 ± 0.9[b]

[d] See Table I for footnotes *a–c*.

Results

The saturated-vapor densities were measured at temperatures above 396 K (0.965 in reduced temperature) and at densities between 181 kg/m^3 (0.407 in reduced density) and 442 kg/m^3, whereas the saturated-liquid densities were measured above 354 K (0.862) and between 446 and 947 kg/m^3 (2.124). The experimental results including 13 saturated-vapor and 18 saturated-liquid densities are listed in Tables I and II.

* To whom correspondence should be addressed.

0021-9568/92/1737-0074$03.00/0

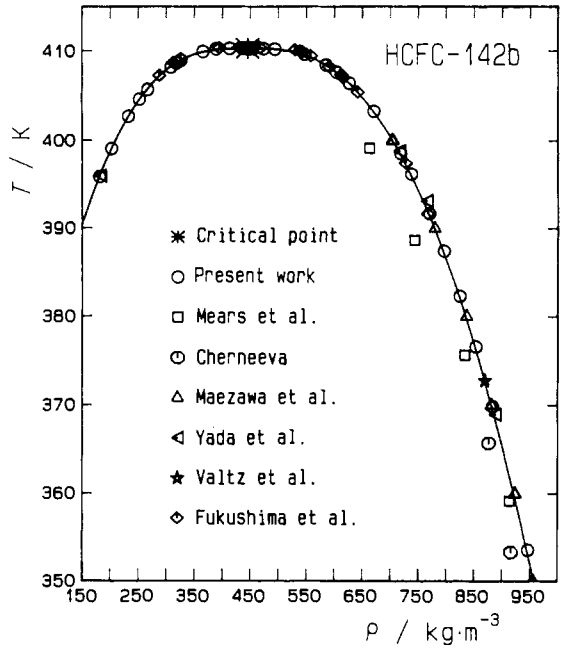

Figure 1. Vapor–liquid coexistence curve of HCFC-142b.

Figure 1 shows the present results on a temperature–density diagram, together with saturation densities at temperatures above 350 K measured by Mears et al. (*7*), Cherneeva (*8*), Valtz et al. (*9*), Fukushima and Watanabe (*10*), Maezawa et al. (*11*), and Yada et al. (*12*). The present results agree with the measurements of Valtz et al. (*9*), Fukushima and Watanabe (*10*), and Maezawa et al. (*11*). The measurements of Yada et al. (*12*) show slightly positive density deviations from the present results for both saturated-vapor and -liquid densities. This seems to us to be due to the difficulty in determining the saturation point near the critical point by the isochoric method employed by Yada et al. (*12*). The measurements of Mears et al. (*7*) and Cherneeva (*8*) are lower than the present results. Such deviations may be partly due to the effect of the sample impurities. The purity of the sample used by Cherneeva was 97%, while Mears et al. did not describe their sample purity.

Critical opalescence was observed for 10 measurements at densities from 365.5 to 493.5 kg/m^3, with corresponding temperatures within 0.34 K of the critical temperature. These measurements are given with an asterisk in Tables I and II. For 11 densities below 412.8 kg/m^3, the meniscus descended with increasing temperature and disappeared at the bottom of the optical cell. For 15 densities above 473.3 kg/m^3, the meniscus ascended with increasing temperature and disappeared at the top of the cell. For the other 5 densities near the critical density, the meniscus disappeared without reaching the top or the bottom of the optical cell. The critical opalescence was observed clearly and more intensely in the liquid phase when the average density was 442.0 kg/m^3; this means that the critical density is larger than this average density. The opalescence, on the other hand, was observed more intensely in the vapor phase when the average density was 453.6 kg/m^3. At 446.0 and 446.8 kg/m^3, the most intense opalescence was observed; we surmized that the critical density should be in between these two density values. Hence, we determined the critical density of HCFC-142b to be ρ_c = 446 ± 3 kg/m^3. The uncertainty of the determination, ±3 kg/m^3, is equivalent to the maximum value of the experimental uncertainty of the density, ±0.53%. The critical temperature should be determined as the saturation temperature corresponding to the critical density. However, as shown in Tables I and II, saturation temperatures of three vapor and four liquid densities coincide to within the experimental uncertainties. Therefore, we determined the critical temperature of HCFC-142b, on the IPTS-68, to be T_c = 410.29 ± 0.02 K. The uncertainty of the determination, ±20 mK, consists of 10 mK for the experimental uncertainty of the temperature and 10 mK for the possible difference in the individual judgments of the disappearance of the meniscus.

Table III. Experimental Critical Parameters of HCFC-142b

ref	method[a]	T_c/K	P_c/MPa	ρ_c/(kg/m^3)
7	1, 2	410.25 ± 0.5	4.12 ± 0.07	435 ± 10
8	1, 2	409.6 ± 0.04	4.192 ± 0.2	427.5 ± 3.5
10	2, 3	410.39 ± 0.03	4.052 ± 0.004	446 ± 5
12	2	(410.29)	4.041 ± 0.002	(446)
present work	3	410.29 ± 0.02		446 ± 3

[a] Methods: (1) extrapolation of the rectilinear diameter; (2) extrapolation of the vapor-pressure correlation; (3) disappearance of the meniscus.

Available measurements of the critical parameters of HCFC-142b are summarized in Table III. The present critical density agrees with that of Fukushima and Watanabe (*10*). The critical density values determined by an extrapolation of the rectilinear diameter by Mears et al. (*7*) and by Cherneeva (*8*) are lower than our value, and these deviations are consistent with the departures of their saturated-liquid densities shown in Figure 1. The present critical temperature agrees with that of Mears et al. (*7*) within the uncertainty, but is larger than that of Cherneeva (*8*) by 0.69 K and smaller than that of Fukushima and Watanabe (*10*) by 0.10 K.

Discussion

The critical exponent, β, is essential for correlating the vapor–liquid coexistence curve in the critical region by means of the following power law representation:

$$(\rho' - \rho'')/2\rho_c = B[(T_c - T)/T_c]^{\beta} \quad (1)$$

where prime and double prime denote the saturated-liquid and -vapor, respectively. B is the critical amplitude. Equation 1 requires isothermal pairs of liquid and vapor densities. However, the present measurements have not been carried out along isotherms. Hence, we used the following correlation as a tool to obtain the isothermal pair densities:

$$(\rho - \rho_c)/\rho_c = 1.7930\tau^{(1-\alpha)} - 1.6108\tau - 0.085644\tau^{(1-\alpha+\Delta_1)} \pm 1.7310\tau^{\beta} \pm 0.69080\tau^{(\beta+\Delta_1)} \quad (2)$$

$$\tau = (T_c - T)/T_c$$

where α and β are the critical exponents. The exponent Δ_1 stands for the first symmetric correction-to-scaling exponent in the Wegner expansion (*13*). From a theoretical background (*13*), these exponents were determined as follows:

$$\alpha = 0.1085, \quad \beta = 0.325, \quad \Delta_1 = 0.50$$

The coefficients in eq 2 were determined by the least-squares fitting of the present measurements, except 9 densities from 389.1 to 493.5 kg/m^3 around the critical point. The upper sign "+" and lower sign "−" of the fourth and fifth terms in eq 2 correspond to the saturated-liquid and -vapor, respectively. The effective density range of eq 2 is between 181 and 947 kg/m^3. The saturation curve calculated from eq 2 is shown in Figure 1. The density deviations of the input data from eq 2 are shown in Figure 2. The deviations of the saturated-liquid densities are shown by open symbols, while those for the saturated vapor by solid symbols, in Figure 2. Equation 2 reproduces the input data within ±0.3%.

Figure 3 shows logarithmic plots in terms of the present measurements and calculated results from eq 2. The power law representation, eq 1, suggests that the present experimental results can be fitted satisfactorily by a straight line. The

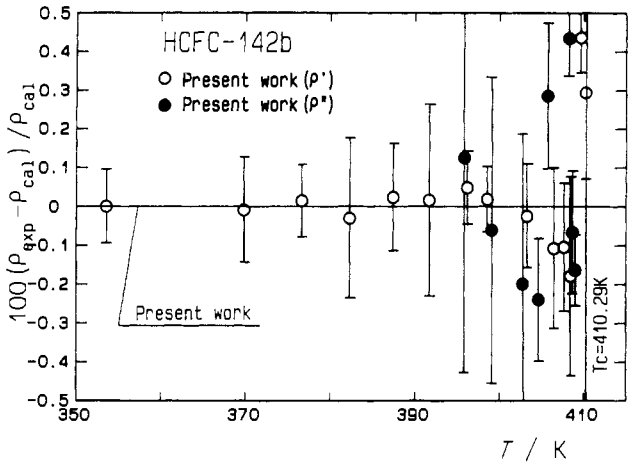

Figure 2. Deviation of the saturated-vapor and -liquid densities from eq 2.

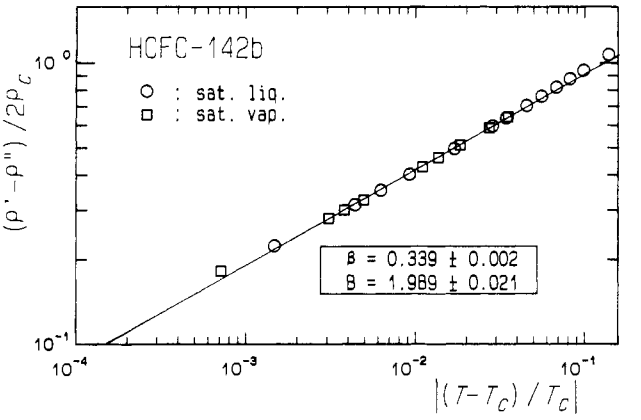

Figure 3. Determination of the critical exponent and amplitude.

slope of the straight line is equivalent to the critical exponent, β. Sixteen measured data at the reduced temperature differences from 0.0007 to 0.037 were used for the determination of the critical exponent, β. β and B were obtained by least-squares fitting as follows:

$$\beta = 0.339 \pm 0.002$$

$$B = 1.989 \pm 0.021$$

where the uncertainties are the standard deviations by the least-squares fitting. For HCFC-142b, the value of the exponent, β, is greater than the theoretical value of 0.325 (*13*), but it is in good agreement with the averaged value of 0.337 with respect to those of six refrigerants determined in our previous measurements (*2*).

On the basis of the present measurements and available saturated-liquid density data reported by Maezawa et al. (*11*), the following correlation was developed:

$$(\rho' - \rho_c)/\rho_c = 1.8375\tau^{0.339} + 0.73070\tau^{0.70} + 0.34987\tau^{3.0} \quad (3)$$

$$\tau = (T_c - T)/T_c$$

As the input data, 49 measurements including 13 present measurements for the densities above 546.0 kg/m^3 and 36 data

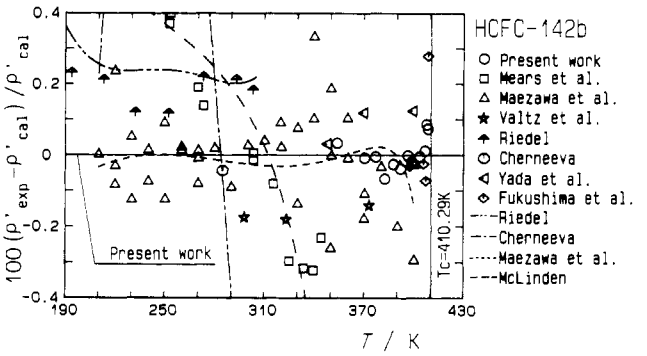

Figure 4. Deviations of the saturated-liquid densities from eq 3.

reported by Maezawa et al. (*11*) were used. The first exponent in eq 3 is the above-mentioned critical exponent, β, while other exponents were determined by trial and error. The coefficients were determined by least-squares fitting. The effective temperature range of eq 3 is between 210 K and the critical temperature. The deviation plots of the input data by Riedel (*14*), Mears et al. (*7*), Cherneeva (*8*), Valtz et al. (*9*), Fukushima and Watanabe (*10*), and Yada et al. (*12*) from eq 3 are shown in Figure 4. The deviations of the saturated liquid density correlations by Riedel (*14*), Cherneeva (*8*), Maezawa et al. (*11*), and McLinden (*15*) from eq 3 are shown in Figure 4. Equation 3 reproduces the input data and most of the other measurements within about ±0.2 or ±0.3%, respectively.

Acknowledgment

We are indebted to Asahi Glass Co. Ltd., Tokyo, and Daikin Industries Ltd., Osaka, for kindly furnishing the samples. We are also indebted to Tokyo Electric Power Co. Ltd., Tokyo, for a grant. The assistance of Tsuneharu Naitoh, who made experiments with us, is gratefully acknowledged.

Registry No. HCFC-142b, 75-68-3.

Literature Cited

(1) Higashi, Y.; Ashizawa, M.; Kabata, Y.; Majima, T.; Uematsu, M.; Watanabe, K. *JSME Int. J.* **1987**, *30* (265), 1106.
(2) Kabata, Y.; Tanikawa, S.; Uematsu, M.; Watanabe, K. *Int. J. Thermophys.* **1989**, *10* (3), 605.
(3) Tanikawa, S.; Kabata, Y.; Sato, H.; Watanabe, K. *J. Chem. Eng. Data* **1990**, *35*, 381.
(4) Okazaki, S.; Higashi, Y.; Takaishi, Y.; Uematsu, M.; Watanabe, K. *Rev. Sci. Intrum.* **1983**, *54* (1), 21.
(5) Higashi, Y.; Okazaki, S.; Takaishi, Y.; Uematsu, M.; Watanabe, K. *J. Chem. Eng. Data* **1984**, *29*, 31.
(6) Higashi, Y.; Uematsu, M.; Watanabe, K. *Trans. JSME* **1985**, *28* (285/286), 2660.
(7) Mears, W. M.; Stahl, R. F.; Orfeo, S. R.; Shair, R. C.; Kells, L. F.; Thompson, W.; McCann, H. *Ind. Eng. Chem.* **1955**, *47* (7), 1449.
(8) Cherneeva, L. I. *Teploenergetika* **1958**, *5* (7), 38.
(9) Valtz, A.; Laugier, S.; Richon, D. *Int. J. Refrig.* **1986**, *9*, 282.
(10) Fukushima, M.; Watanabe, N. *Preprints of the JSME Thermal Engineering Conference '90*, Sapporo, Japan, 1990; JSME: Tokyo, 1990; No. 900-71, p 3.
(11) Maezawa, Y.; Sato, H.; Watanabe, K. *J. Chem. Eng. Data* **1991**, *36*, 148.
(12) Yada, N.; Kumagai, K.; Tamatsu, T.; Sato, H.; Watanabe, K. *J. Chem. Eng. Data* **1991**, *36*, 12.
(13) Levelt Sengers, J. M. H.; Sengers, J. V. *Perspectives in Statistical Physics*, Raveche H. J., Ed.; North-Holland: Amsterdam, 1981; Chapter 14.
(14) Riedel, L. Z. *Gesamte Kälte-Ind.* **1941**, *48* (7), 105.
(15) McLinden, M. O. *Int. J. Refrig.* **1990**, *13*, 149.

Received for review March 20, 1991. Accepted September 10, 1991.